

Thermodynamic Assessment of the Partitioning of Acetone between Supercritical CO₂ and Polystyrene Using the Polar PC-SAFT Equation of State

Ali A. AlHammadi* and Mohammed I. L. Abutaqiya



Cite This: *ACS Omega* 2020, 5, 29530–29537



Read Online

ACCESS |



Metrics & More

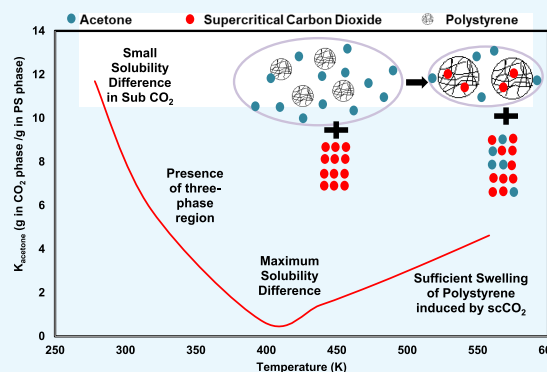


Article Recommendations



Supporting Information

ABSTRACT: Supercritical carbon dioxide (scCO₂) has gained considerable attention in the process industry due to its favorable economic, environmental, and technical characteristics. Polymer processing is one of the key industrial applications where scCO₂ plays an important role. In order to be able to efficiently design the polymer processing equipment, understanding the phase behavior and partition of solutes between scCO₂ and polymers is necessary. This paper investigates the partitioning of acetone – a conventional polar cosolvent – between scCO₂ and polystyrene – a glassy polymer. We highlight the importance of taking into account the polar interactions between acetone molecules and their role in the polymer phase behavior. The system is modeled under a wide range of temperatures and pressures (278.15–518.2 K and 1.0–20.0 MPa) using the polar version of the perturbed chain statistical associating fluid theory (polar PC-SAFT) equation of state. The results show that at relatively low pressure, the system exhibits a vapor–liquid–liquid (VLL) three-phase region bounded by two two-phase regions (VL and LL). At high pressure, VLL and VL regions disappear and only the LL region remains. The temperature effect is more interesting, showing a transition of upper critical solution temperature behavior to lower critical solution temperature behavior at 10 MPa and 398.15 K. It is found that neglecting the polar term can lead to significant changes in the description of the polymeric-system phase behavior especially at lower temperatures. No such differences are observed at higher temperatures (above 500 K) where the effect of polar interaction is considerably weaker.



INTRODUCTION

The special characteristics of supercritical carbon dioxide (scCO₂), such as nontoxicity, chemical inertness,¹ high diffusivity, and considerable solvation power,² have allowed its wide application in the chemical and processing industry. These processes include particle formation, reaction,³ fractionation,⁴ purification, extraction, drying,⁵ blending, foaming,⁶ and developing polymer complexes.^{7–9} In many cases, practical applications of scCO₂ have not only been studied but also realized.^{10,11}

In extraction and impregnation processes, knowledge of the phase equilibrium and partitioning of a solute between the fluid and polymer phases is a key parameter for design. Despite the limited solubility of polymers in carbon dioxide (CO₂), carbon dioxide has considerable solubility in many polymers. Such high solvent power ends up swelling the polymer matrix.^{12,13} scCO₂ swells glassy polymers, enabling incorporation of additives. The degree of polymer swelling and consequently its free volume can be changed merely by varying the density of scCO₂, which can be controlled with pressure and temperature. Therefore, knowledge of phase behavior conditions is key for fine tuning the solute amount partitioned

and diffused between the swollen-polymer phase and the fluid phase.¹⁴

Kazarian et al.¹⁴ used in-situ Fourier transform infrared and UV–vis spectroscopy to measure the partition of azo dyes and deuterated water between scCO₂ and polymer phases, thus providing experimental data for the modeling of fluid extractions. Schnitzler and Eggers¹⁵ measured the swelling of polymers in scCO₂ as part of their study of the diffusion behavior in the polymers and concluded that this swelling reduces the resistance and enables faster diffusion into the polymer matrix. Kiran¹⁶ experimentally measured the miscibility of poly(L-lactic acid) in a binary mixture of carbon dioxide and acetone. As expected, at low pressure, the polymer was not soluble. However, as pressure increased to 60 MPa, it became completely soluble. Gutiérrez et al.¹⁷ used the

Received: September 13, 2020

Accepted: October 20, 2020

Published: November 3, 2020



semiempirical correlation of Chrastil's equation and dual-mode model to model the solubility of polystyrene in p-cymene and carbon dioxide.

Lee et al.¹⁸ and Ji¹⁹ used Peng-Robinson (PR) and Soave-Redlich-Kwong (SRK) equations of state, respectively, with some success in order to describe the phase behavior of many systems containing carbon dioxide and polymers. Despite their simplicity and its frequent use in industry, cubic equations of state are not the most suitable for polymer modeling because the molecules in a cubic EOS are treated as interacting spheres. This assumption is not expected to be representative of polymer systems, which are rather large chain molecules.

Other more popular approaches are association equations of state and lattice models, which gained more popularity after the work of Flory and Huggins in modeling polymer systems.²⁰ Kontogeorgis et al. used a simplified cubic plus association equation of state to estimate the vapor–liquid equilibria for different polymers with solvent systems.²¹ Panayiotou et al. used the nonrandom hydrogen bonding lattice theory successfully, which is known for its strong interaction applicability to model the phase behavior of polymers and organic liquids with solvent systems.^{22,23} The popularity of lattice fluid models such as Sanchez Lacombe (SL) and Associated Lattice Fluid (ALF) comes from their practicality following the minimum number of binary parameters, compared to cubic equations of state. However, there is a lack of data to estimate the parameters needed for the lattice model especially on systems such as carbon dioxide with polymers. Therefore, experimental spectroscopic data and NMR measurements as well as quantum calculations to obtain lattice fluid model parameters are definitely recommended.²⁰

Lotfollahi et al. modeled hydrocarbon–polymer–scCO₂ using the SL model and compared it with the perturbed hard sphere chain (PHSC) model. The authors recommended the SL model over the PHSC model based on the complexity and speed of calculations. The PHSC theory was proposed by Song et al.²⁴ and provides good approximations for various associating and nonassociating components of which carbon dioxide and polymer systems can be used. On the other hand, statistical associating fluid theory (SAFT) models have proven to be somewhat superb, compared to it.²⁵

The SAFT equation of state was proposed by Chapman et al.^{26,27} based on Wertheim's theory.^{28–31} Its ability to accurately predict phase splitting in systems with large variations of size and shape made it one of the most widely used equations of state.^{32–34} Tremendous success has been shown^{33,35–38} in modeling phase behavior of systems of large size differences such as polymers and asphaltene using the SAFT equation of state and its variations (e.g., PC-SAFT³⁹). These include systems of complex interaction mixtures of associating and nonassociating components.^{40–42} Examples are the work of Aghaie et al.⁴³ and Kondori et al.⁴⁴ where they used the PC-SAFT equation of state to model CO₂ solubility in ionic liquids⁴³ and to evaluate gas hydrates.⁴⁴ They also compared PC-SAFT results to extended PR and UNIQUAC and concluded that PC-SAFT was superior in its accuracy.

In SAFT, associating molecule free energies are defined based on a reference fluid with energy contributions from hard spherical segments, along with energies of chain formation, Van der Waals dispersion, and association terms such as hydrogen bonding. Molecules are originally constructed as chains of hard spheres that are connected through covalent bonds.⁴⁵ The fluid properties can be calculated by the

contribution coming from the chain formation, Van der Waals dispersion forces, and hydrogen bonding based on the perturbation theory.⁴⁶ For molecules with polar interactions, a polar term can be also added. Several variations of SAFT have been proposed over the years.^{39,47–50} Of particular interest is the perturbed chain variation of SAFT (PC-SAFT) developed by Gross and Sadowski.³⁹ PC-SAFT is favored over other variations mainly due to its availability in commercial simulators, such as VLXE/IBLEND of VLXE ApS,⁵¹ Multiflash of KBC-Yokogawa,⁵² and PVTsim of Calsep.⁵³

In this work, the partition coefficients of acetone between compressed carbon dioxide and polystyrene are modeled using the Polar PC-SAFT equation of state for conditions of 278.15–518.2 K and up to 20.0 MPa. Acetone is a conventional cosolvent with polar–polar interactions. It can improve the limited solubility of polymers and other potential solute in carbon dioxide while competing with other solutes in the polymer phase.⁵⁴ The polymer of choice is polystyrene (PS), a glassy and nonadsorbing polymer. This study presents an analysis of the contributing factors that may influence the phase behavior and partitioning of acetone in such polymer systems. Additionally, the effect of the polar–polar interactions of acetone on the polymer phase behavior is highlighted.

METHODOLOGY

The system studied here is a complex mixture of PS, carbon dioxide, and acetone where PS constitutes a nonadsorbing polymer, acetone is the polar solute, and scCO₂ is the solvent. This system is modeled using the polar version of the PC-SAFT equation of state as proposed by Dominik et al.⁵⁵ The polar PC-SAFT can be described by the residual Helmholtz free energy as

$$A^{\text{res}} = A^{\text{hs}} + A^{\text{chain}} + A^{\text{disp}} + A^{\text{assoc}} + A^{\text{polar}}$$

The system studied here is nonassociating, and therefore, the associating term (A^{assoc}) can be neglected. The remaining terms include the hard sphere (A^{hs}), the chain formation (A^{chain}), the dispersion energy (A^{disp}), and polar interactions (A^{polar}). A detailed analysis of these various terms and their calculations included in polar PC-SAFT can be found elsewhere.^{27,35,55,56}

The PC-SAFT parameters of the different components (other than acetone) were obtained from Gross and Sadowski^{39,57} and are summarized in Table 1. The association term

Table 1. PC-SAFT Parameters for the Model System Obtained from Gross and Sadowski^{39,57a}

component	MW [g/mol]	m/MW [mol/g]	σ [Å]	ϵ/k [K]
CO ₂	44.01	0.0471	2.785	169.21
acetone	58.08	0.0382	3.608	259.99
polystyrene	400,000	0.0190	4.107	267.00

^aAcetone is polar with a polarity of 0.2258 and dipole moment of 2.7 D. Association is neglected for all components

in PC-SAFT is neglected for all components studied in this work since they are nonassociating. The polar term is included for acetone, with a polarity of 0.2258 and dipole moment of 2.7 D.⁵¹

In order to model the ternary system accurately, the available binary systems of carbon dioxide–acetone and carbon dioxide–PS were modeled first to obtain the binary interaction parameters. The vapor–liquid phase behavior of both binary

systems based on the experimental data^{58–60} can be found in the Supporting Information. The binary interaction coefficient (k_{ij}) between acetone and carbon dioxide is found to be zero. On the other hand, k_{ij} between carbon dioxide and PS was found to be 0.2. The k_{ij} between acetone and PS was fitted to the partition behavior of acetone at $T = 318.15$ K and a PS MW of 400,000 g/mol. Note that such high k_{ij} values for systems containing heavy polymer-like components and CO₂ were previously reported in the literature.^{61,62} In fact, Arya et al.⁶¹ showed that using low k_{ij} values for asphaltenes–CO₂ leads to unphysical crossover behavior from PC-SAFT when modeling liquid–liquid equilibria (LLE) of asphaltene precipitation in crude oils. The authors recommended a k_{ij} of 0.19. Given the similarity in the framework of modeling asphaltenes and polymers as liquid–liquid phase separation, the obtained k_{ij} in this work seems reasonable. Based on these parameters, the phase behavior of the ternary system can now be modeled using polar PC-SAFT at different pressures and temperatures. A sensitivity analysis on these parameters showed that all effects on overall accuracy can be offset with slight tuning of the binary interaction parameter.

RESULTS AND DISCUSSION

For the system of PS and acetone, the data were limited, and the binary interaction coefficient varied with molecular weight ranges. The system of solute–polymer in compressed carbon dioxide was found to be of interest as it is important to understand how the solute will partition between compressed carbon dioxide and polymer-rich phases for the efficient design of polymer separation and extraction processes. Based on the binary phase diagram modeling and for simplicity, the binary interaction coefficient between carbon dioxide and acetone is set to zero and between the polymer and carbon dioxide is set to 0.2. The binary interaction coefficient between the solute and polymer was fitted to a set of experimental partition data from He and Wang.⁵⁴ The optimized set of binary interaction parameters along with error analysis is summarized in Table 2. Overall, PC-SAFT can capture the experimental data with reasonable accuracy and an average absolute percent deviation (AAPD%) of around 5–10%. The vast majority of data are

Table 2. Binary Interaction Parameters k_{ij} between Solutes and Polymers Were Fitted to Different Partition Data^a

	binary interaction parameter (k_{ij})		
	PS	PC	PMMA
MMA	−0.024	−0.065	−0.044
acetone	−0.042	−0.053	−0.022
average absolute percentage deviation (AAPD%)			
	PS	PC	PMMA
MMA	9.4	7.6	17.7
acetone	6.7	5.8	5.8
maximum absolute percentage deviation (max APD%)			
	PS	PC	PMMA
MMA	15.3	11.9	72.2
acetone	10.1	9.6	11.5

^aThe k_{ij} between the solute and CO₂ is 0 and between polymers and CO₂ is 0.2 in all systems. More information regarding how the k_{ij} values were obtained can be found in the Supplementary Information. The average absolute percent deviation (AAPD%) and maximum absolute percent deviation (Max APD%) for the systems are presented in Figures 1 and 2

within 5% error in all cases. However, for the system containing CO₂, methylmethacrylate, and polymethylmethacrylate (PMMA), the error is relatively larger due to the peculiar experimental data. The solutes are acetone and methylmethacrylate (MMA), and the polymers are polycarbonate (PC), PS, and PMMA. The partition coefficient (K_i) results for different solutes and polymers in compressed carbon dioxide are modeled at 318.15 K. These results are shown in Figures 1 and 2 where the solutes are acetone and MMA, respectively.

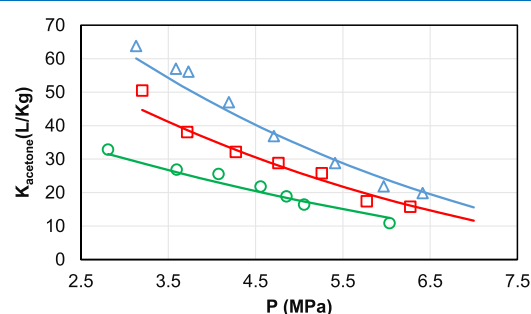


Figure 1. Partition coefficient of acetone between the polymer and compressed carbon dioxide at 318.15 K. The solid lines are PC-SAFT prediction, and experimental values are labeled as follows: triangles, polycarbonate; squares, polymethylmethacrylate; circles, polystyrene. Experimental data are from He and Wang.⁵⁴

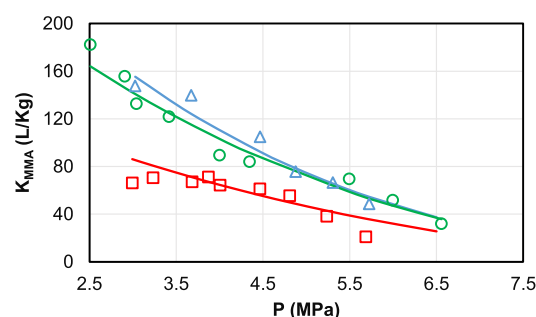


Figure 2. Partition coefficient of methylmethacrylate between the polymer and compressed carbon dioxide at 318.15 K. The solid lines are PC-SAFT prediction, and experimental values are labeled as follows: triangles, polycarbonate; squares, polymethylmethacrylate; and circles, polystyrene. Experimental data are from He and Wang.⁵⁴

It is clear that at constant temperature, the partition coefficient of the solute represented here by acetone and MMA decreases sharply with pressure for all polymers studied. This is possibly due to the pressure effect on carbon dioxide. At higher pressure, the solute tends to dissolve easily in carbon dioxide. On the other side, compressed carbon dioxide competes with the solute while swelling the polymer matrix. In addition to the pressure, both the polymer and the solute play distinctive roles in how the solute partitions between the polymer and compressed carbon dioxide. Modeling of phase behavior is typically a challenge. In this case, we choose one of the systems to represent the modeling behavior of the associating solute–polymer–CO₂ system. The system of choice is acetone–PS–carbon dioxide.

Despite acetone being moderately polar, the effectiveness of the polar term is mainly a function of other components and the variation in molecular sizes and interactions. Figure 3

illustrates the effect of including the polar term on the phase behavior of the acetone–PS–carbon dioxide system.

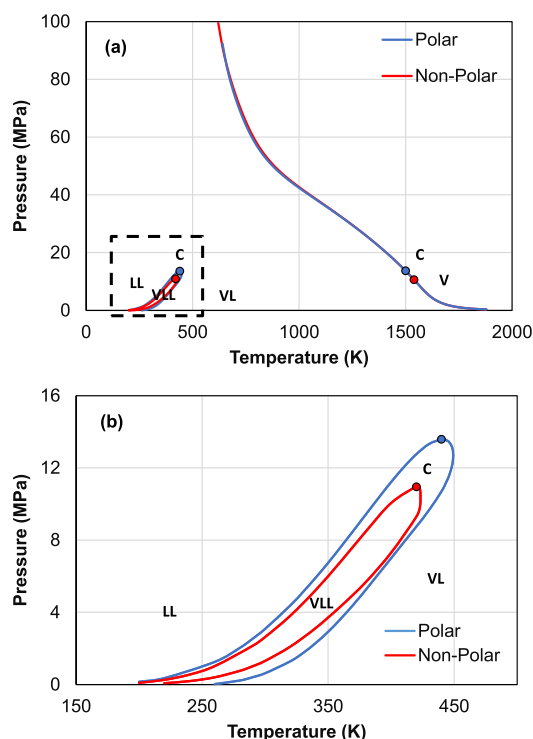


Figure 3. Pressure–Temperature phase behavior of acetone–polystyrene–carbon dioxide (33.3 wt % each). **Figure 3.a** shows the PT phase diagram to high temperature and pressure, and **Figure 3.b** focuses on the three-phase region of VLL. The three phases are polymer-rich liquid, CO₂-rich liquid, and vapor phases.

From **Figure 3**, we can deduce that including the polar term of acetone affects the overall phase behavior of this system. This effect is clearer at lower temperature as can be seen from the three-phase region. The polar term here causes a larger region of the vapor–liquid–liquid (VLL). Moreover, there is a shift in the critical points.

The critical pressure and temperature of carbon dioxide is 7.377 MPa and 304.1 K, respectively. Therefore, it would be of interest to look at the effect of pressure and temperature as carbon dioxide transitions through its critical point. The effect of the pressure on the equilibrium boundary line is shown in **Figure 4**.

The boundary condition does not vary much with variations in pressure. The system transitions between the one-liquid phase and multiphases depending on the pressure. At a lower pressure of 1 MPa, the two-phase region is larger due to the presence of the gaseous carbon dioxide phase. However, as carbon dioxide reaches the supercritical state, it dissolves easily into the polymeric phase, thus expanding the one-phase region. Above the critical pressure, the phase behavior was not sensitive to increasing pressure. The boundary lines indicate that the acetone–PS binary system will always form one liquid phase, while addition of carbon dioxide induces phase separation. A detailed look at the ternary phase diagram of the acetone–PS–carbon dioxide system and tie lines is demonstrated below, starting from 1 MPa in **Figure 5**.

The regions above are two-phase regions of carbon dioxide-rich gas and polymer-rich liquid phases. Increasing the pressure

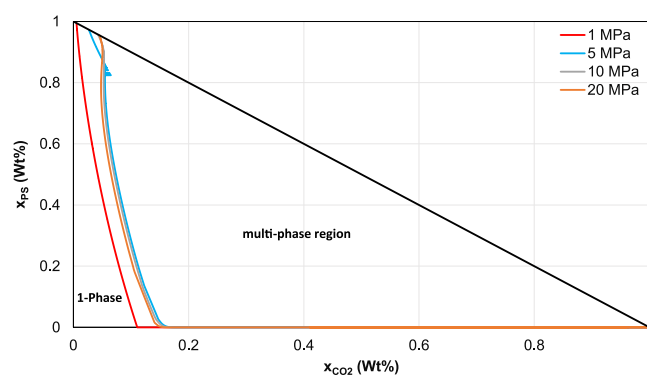


Figure 4. Ternary phase behavior of acetone–polystyrene–carbon dioxide at 318.15 K and different pressures. The one-phase region expands as the supercritical CO₂ is reached, above which it does not vary with increasing pressure.

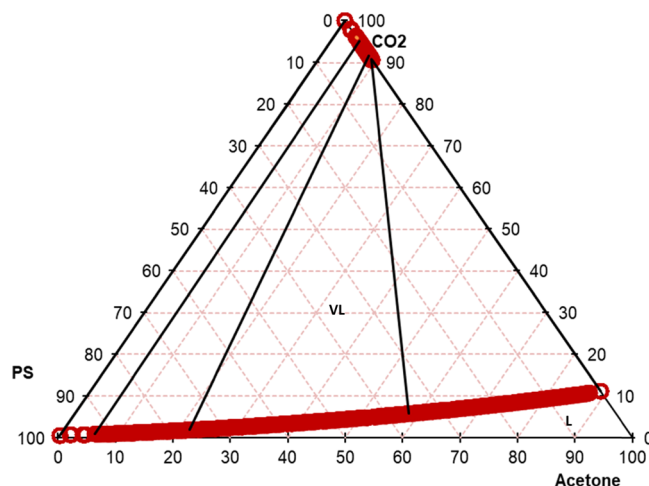


Figure 5. Ternary phase behavior of acetone–polystyrene–carbon dioxide at 318.15 K and 1 MPa. The graph shows the boundary lines and tie lines connecting the liquid polymer-rich phase with a gaseous carbon dioxide-rich phase.

will result in a shift toward three phases of VLL equilibrium as can be seen from **Figure 6** at 3 MPa and 318.15 K.

The blue region is a three-phase region of VLL. To its left, the region is vapor–liquid and to the right and below, the region is liquid–liquid. Increasing the pressure will cause a decrease in the size of the vapor–liquid region and an increase of the two phases of liquid–liquid equilibria, thus decreasing the size of the three-phase region of VLL as can be seen from **Figure 7**.

As noticed, as carbon dioxide is pressurized, the vapor–liquid and the VLL regions shrink, as visible from both the graph and tie lines. This shrinking continues, as the supercritical state of carbon dioxide is reached. Under these conditions, the system phase separates into carbon dioxide-rich and PS-rich phases, which is clear from **Figure 8**.

Despite the boundary line being almost constant, the type of boundary changes. At a low pressure of 1 MPa, the region entirely consists of two phases, which are vapor and liquid. At a high pressure of above 9 MPa, the VL region disappears, and the phase diagram consists of a one-miscible-liquid-phase region and a two-immiscible-liquid-phase region. In between, there is a transition of three phases (VLL) visualized by the change of the vapor–liquid–liquid equilibria (VLLE) region.

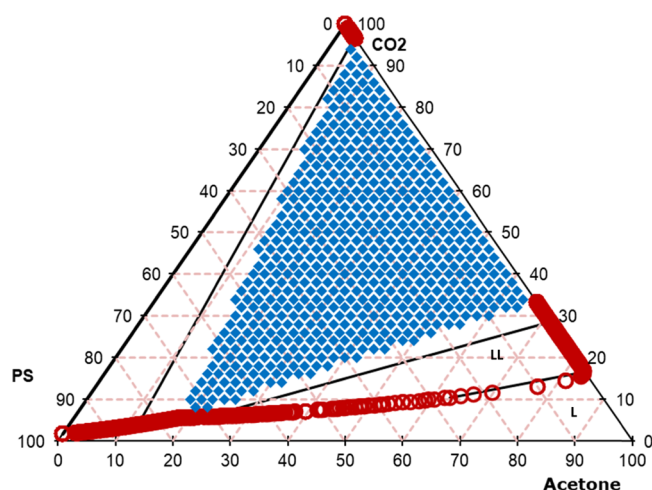


Figure 6. Ternary phase behavior of acetone–polystyrene–carbon dioxide at 318.15 K and 3 MPa. The red circles indicate two-phase regions, while the blue rectangles indicate the three-phase regions. The VLL three-phase region is bounded by two two-phase regions (VL and LL)

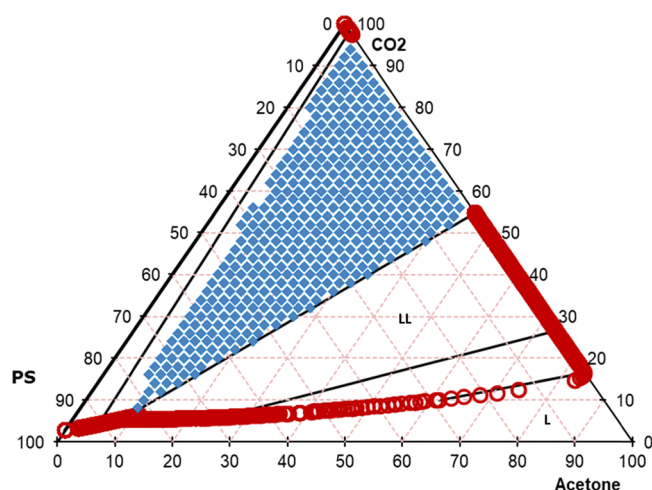


Figure 7. Ternary phase behavior of acetone–polystyrene–carbon dioxide at 318.15 K and 5 MPa. The red circles indicate two-phase regions, while the blue rectangles indicate the three-phase regions. As the pressure increases, the size of the three-phase region shrinks.

At higher pressure, the behavior stays consistent as shown in Figure 4. More details on the pressure effect can be found in the supporting documents.

The effect of temperature is more pronounced and categorizes under two different ranges. As temperature increases from 278.15 to 398.15 K, more carbon dioxide mixes in the single-phase liquid, causing the one-phase region to expand. This happens due to different contributing factors. At 278.15 K and 10 MPa, carbon dioxide is in the subcritical liquid region. Therefore, the slightest presence of CO₂ causes a phase separation into polymeric-rich and CO₂-rich phases. At 318.15 K and 10 MPa, carbon dioxide is already in the supercritical region and is able to dissolve in the PS phase. This effect continues causing the one-phase region to expand as visible from the solid lines in Figure 9.

However, above 398.2 K, the single-phase region shrinks as visible from the dashed lines. This can be better explained by

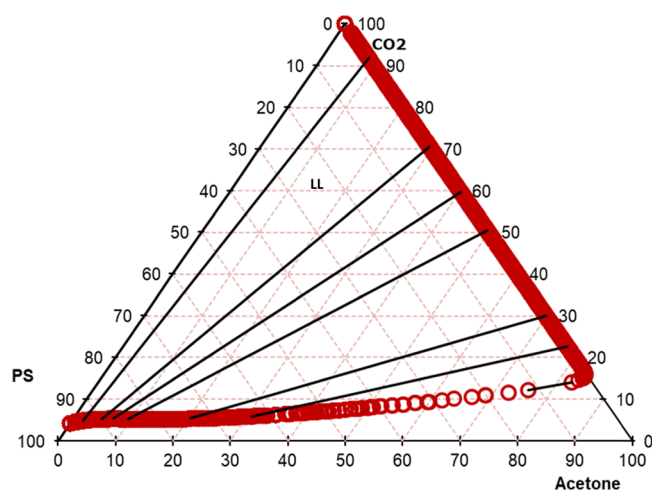


Figure 8. Ternary phase behavior of acetone–polystyrene–carbon dioxide at 318.15 K and 10 MPa. The circles indicate the liquid–liquid equilibrium. In these conditions of scCO₂, the system phase separates into CO₂-rich and polymer-rich phases. The tie lines are represented inside the two-phase regions. Acetone and polystyrene are completely miscible at this pressure and temperature.

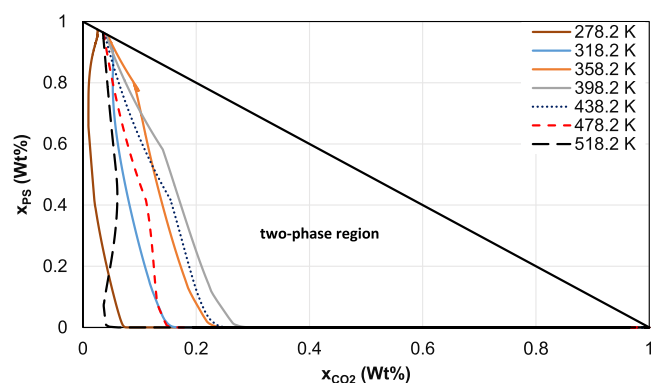


Figure 9. Ternary phase behavior of acetone–polystyrene–carbon dioxide at 10 MPa and different temperatures. The one-phase region expands as the supercritical CO₂ is reached until 398.15 K, above which it shrinks due to large difference in the solubility parameter.

how the solubility parameter of the different components changes with temperature as shown in Figure 10 below.

The solubility parameter of carbon dioxide is closer to PS and acetone at lower temperatures. As the temperature increases to 398.15 K, the effect of solvation of scCO₂ is dominant. However, as the difference between CO₂ and both acetone and PS is maximum at such a temperature, the three-phase region is more notable. On the other hand, as the temperature increases above 398.15 K, the solubility parameter of acetone gets closer to scCO₂ causing the three-phase region to shrink and more acetone to partition in the scCO₂ as demonstrated in Figure 11. The phase diagram of the ternary system at the temperature ranges of 278.15 to 518.15 K is available in the supporting documents. Another important observation is the effect of the polar term. Nonpolar acetone has closer solubility to CO₂ and PS, which helps explain the smaller VLL region in Figure 3.

As clear from previous graphs, knowledge of the solubility parameter, partition coefficients, and ternary phase behavior are key in determining the most suitable conditions for separation purposes. The partition coefficient of acetone

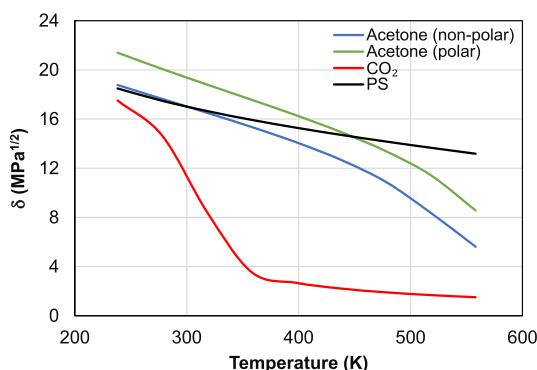


Figure 10. Solubility parameter of acetone, polystyrene, and carbon dioxide at 10 MPa and different temperatures. Blue line, acetone (polar term not included); green line, acetone (polar term included); red line, carbon dioxide; and black line, polystyrene. At lower temperature, the solubility parameters of the three components are similar. At high temperatures, acetone tends to partition in scCO_2 .

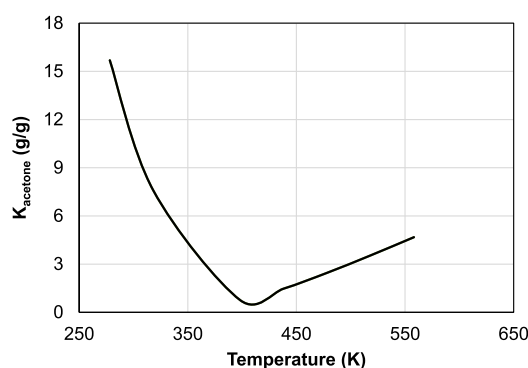


Figure 11. Partition Coefficient of acetone in the CO_2 -rich phase compared to the polystyrene-rich phase at 10 MPa. At low temperature, acetone partitions in supercritical carbon dioxide.

between scCO_2 and PS is a strong function of temperature, which directly impacts how the compressed carbon dioxide behaves in subcritical liquid and supercritical states. Another important deduction from the interesting behavior of temperature effects is the one region expansion and shrinking. Figure 11 shows the partition coefficient of acetone at constant pressure; thus, at constant composition, we can deduce the type of system behavior. Comparing temperatures such as 318.15 and 398.15 K, there are many two-phase compositions at 318.15 K that have become one phase at 398.15 K. This indicates an upper critical solution temperature (UCST) behavior. However, above such a temperature, there are many single-phase compositions at 398.15 K that went through phase separation at 518.15 K, indicating a lower critical solution temperature (LCST) behavior. This means that there was a transition from UCST to LCST behavior. At higher temperatures, the increase of scCO_2 solvent power means a higher swelling effect on the PS matrix causing a weakening of acetone attachment to the polymer phase. Therefore, acetone tends to partition more toward the scCO_2 -rich phase. Similar partition and phase behavior results were obtained for acetone and MAA in scCO_2 and other polymers (PC, PS, and PMMA). Depending on the application of interest, different aspects of the phase behavior described above can be used (e.g., blending of additives would require understanding polymer swelling by incorporating scCO_2).

CONCLUSIONS

The knowledge of the partition of solutes in supercritical solvents and polymers is critical for applications including separation, extraction, pharmaceuticals, and chemical reactions. In this work, the polar PC-SAFT equation of state was applied successfully to model the partitioning of acetone between compressed carbon dioxide and PS at different pressures and temperatures. The high accuracy of PC-SAFT EoS is attributed to its strong theoretical basis and rigorous incorporation of molecular interaction and size effects. Such features are key when modeling systems with large size differences and complex molecular interactions.

As acetone is moderately polar, including the polar term is necessary for an accurate description of the phase behavior and excess properties. While the system experimental data are lacking, the effect of including the polar term is clear. The polar term increased the VLL region and had less effect at higher temperature. Moreover, the system of interest includes components with various sizes and intermolecular forces. This includes the tricky scCO_2 , the polar solvent of acetone, and comparably large-size PS.

The partition coefficient of acetone was affected by many factors, including the polymer type and molecular weight, pressure, and temperature. At a constant temperature of 318.15 K, the partition coefficient decreased with increasing pressure for the different polymers. A main factor was the transition of carbon dioxide from the gaseous to supercritical state. A three-phase region of VLL emerged as carbon dioxide is pressurized.

The effect of temperature demonstrated interesting behavior as the carbon dioxide transitioned from the subcritical to supercritical state. At a constant pressure of 10 MPa, the partition coefficient went through a minimum as temperature increased, indicating that acetone tends to partition more into carbon dioxide phases at low and high temperatures. Therefore, a complete analysis of the phase behavior is useful when designing an efficient separator. A transition from UCST behavior to LCST behavior was observed around 398.15 K and 10 MPa. Many factors may contribute to the behaviors observed in this study. These include how the solubility parameter changes for the different components, the competition of carbon dioxide with the solute in the polymer phase, and the swelling behavior in the polymer phase induced by the presence of carbon dioxide. A detailed design study needs to be conducted for analyzing the acetone– CO_2 –PS system with phase behavior results generated from polar PC-SAFT in order to understand the extent of applicability of the proposed modeling work.

ASSOCIATED CONTENT

Supporting Information

The Supporting Information is available free of charge at <https://pubs.acs.org/doi/10.1021/acsomega.0c04487>.

Summary of the binary VLE fitting for the binary interactions and the effect of temperature and pressure on the phase behavior of acetone– scCO_2 –polystyrene (PDF).

AUTHOR INFORMATION

Corresponding Author

Ali A. AlHammadi – Department of Chemical Engineering and Center for Catalysis and Separation, Khalifa University of Science and Technology, Abu Dhabi, United Arab Emirates;

orcid.org/0000-0002-2747-2492; Email: ali.aalhammadi@ku.ac.ae

Author

Mohammed I. L. Abutaqiya – ENNOVA LLC, Stafford, Texas 77477, United States; orcid.org/0000-0002-7161-0733

Complete contact information is available at:

<https://pubs.acs.org/10.1021/acsomega.0c04487>

Notes

The authors declare no competing financial interest.

ACKNOWLEDGMENTS

A.A.A. acknowledges the financial support from Khalifa University under the RCII-2018-024.

REFERENCES

- (1) Wu, K.; Li, J. Precipitation of a Biodegradable Polymer Using Compressed Carbon Dioxide as Antisolvent. *J. Supercrit. Fluids* **2008**, *46*, 211–216.
- (2) Jafari, N. S.; Abolghasemi, H.; Moosavian, M. A.; Maragheh, M. G. Prediction of Solute Solubility in Supercritical Carbon Dioxide: A Novel Semi-Empirical Model. *Chem. Eng. Res. Des.* **2010**, *88*, 893–898.
- (3) Kazarian, S. G. *Polymer Processing with Supercritical Fluids*; 2000, 42.
- (4) Wang, Y.; Dave, R. N.; Pfeffer, R. Polymer Coating/Encapsulation of Nanoparticles Using a Supercritical Anti-Solvent Process. *J. Supercrit. Fluids* **2004**, *28*, 85–99.
- (5) Meconi, G. M.; Tomovska, R.; Zangi, R. Adsorption of CO₂ Gas on Graphene–Polymer Composites. *J. CO₂ Util.* **2019**, *32*, 92–105.
- (6) Goimil, L.; Jaeger, P.; Ardao, I. L.; Gómez-Amoza, J. L.; Concheiro, A.; Alvarez-Lorenzo, C.; Garcia-Gonzalez, C. A. Preparation and Stability of Dexamethasone-Loaded Polymeric Scaffolds for Bone Regeneration Processed by Compressed CO₂ Foaming. *J. CO₂ Util.* **2018**, *24*, 89–98.
- (7) Sun, Y. *Supercritical Fluid Technology in Materials Science and Engineering: Syntheses: Properties, and Applications*; 2002.
- (8) Shariati, A.; Omidkhah, M.; Pedram, M. Z. New Permeation Models for Nanocomposite Polymeric Membranes Filled with Nonporous Particles. *Chem. Eng. Res. Des.* **2012**, *90*, S63–S75.
- (9) Baldino, L.; Cardea, S.; Reverchon, E. A. Supercritical CO₂ Assisted Electrohydrodynamic Process Used to Produce Micro-particles and Microfibers of a Model Polymer. *J. CO₂ Util.* **2019**, *33*, S32–S40.
- (10) Matsukawa, H.; Shimada, Y.; Yoda, S.; Okawa, Y.; Masakazu, N.; Shono, A.; Otake, K. Phase Behavior of Carbon Dioxide/Tetramethyl Orthosilicate/Polymer Ternary Systems. *Fluid Phase Equilib.* **2018**, *457*, 1–10.
- (11) Zheng, H.; Zhang, J.; Yan, J.; Zheng, L. An Industrial Scale Multiple Supercritical Carbon Dioxide Apparatus and Its Eco-Friendly Dyeing Production. *J. CO₂ Util.* **2016**, *16*, 272–281.
- (12) Said, A. B.; Guinot, C.; Ruiz, J. C.; Grandjean, A.; Dole, P.; Joly, C.; Chalamet, Y. Modeling of Supercritical CO₂ Extraction of Contaminants from Post-Consumer Polypropylene: Solubilities and Diffusion Coefficients in Swollen Polymer at Varying. *Chem. Eng. Res. Des.* **2017**, *117*, 95–109.
- (13) Han, Y.; Zheng, H.; Jing, X.; Zheng, L. Swelling Behavior of Polyester in Supercritical Carbon Dioxide. *J. CO₂ Util.* **2018**, *26*, 45–51.
- (14) Kazarian, S. G.; Vincent, M. F.; West, B. L.; Eckert, C. A. Partitioning of Solutes and Cosolvents between Supercritical CO₂ and Polymer Phases. *J. Supercrit. Fluids* **1998**, *13*, 107–112.
- (15) von Schnitzler, J.; Eggers, R. Mass Transfer in Polymers in a Supercritical CO₂-Atmosphere. *J. Supercrit. Fluids* **1999**, *16*, 81–92.
- (16) Kiran, E. Foaming Strategies for Bioabsorbable Polymers in Supercritical Fluid Mixtures. Part I. Miscibility and Foaming of Poly (L-Lactic Acid) in Carbon Dioxide+ Acetone Binary. *J. Supercrit. Fluids* **2010**, *54*, 296–307.
- (17) Gutiérrez, C.; Rodríguez, J. F.; Gracia, I.; de Lucas, A.; Garcia, M. T. Determination of the High-Pressure Phase Equilibria of Polystyrene/p-Cymene in Presence of CO₂. *J. Supercrit. Fluids* **2014**, *92*, 288–298.
- (18) Lee, H. Y.; Yoon, S. D.; Byun, H. S. Cloud-Point and Vapor-Liquid Behavior of Binary and Ternary Systems for the Poly(Dodecyl Acrylate) + Cosolvent and Dodecyl Acrylate in Supercritical Solvents. *J. Chem. Eng. Data* **2010**, *55*, 3684–3689.
- (19) Ji, W. Modeling VLE and GLE of Systems Involving Polymers by Using SRK Equation of State. *Chin. J. Chem. Eng.* **2007**, *15*, 221–227.
- (20) Hossain, M. Z.; Teja, A. S. Modeling Phase Equilibria in CO₂+ Polymer Systems. *J. Supercrit. Fluids* **2015**, *96*, 313–323.
- (21) Kontogeorgis, G. M.; Yakoumis, I. V.; Vlamos, P. M. Application of the SCPA Equation of State for Polymer Solutions. *Comput. Theor. Polym. Sci.* **2000**, *10*, S01–S06.
- (22) Panayiotou, C.; Tsivintzelis, I.; Economou, I. G. Nonrandom Hydrogen-Bonding Model of Fluids and Their Mixtures. 2. Multi-component Mixtures. *Ind. Eng. Chem. Res.* **2007**, *46*, 2628–2636.
- (23) Pantoula, M.; Panayiotou, C. Sorption and Swelling in Glassy Polymer/Carbon Dioxide Systems: Part I. Sorption. *J. Supercrit. Fluids* **2006**, *37*, 254–262.
- (24) Song, Y.; Lambert, S. M.; Prausnitz, J. M. A Perturbed Hard-Sphere-Chain Equation of State for Normal Fluids and Polymers. *Ind. Eng. Chem. Res.* **1994**, *33*, 1047–1057.
- (25) Prausnitz, J.; Lichtenthaler, R.; de Azevedo, E. *Molecular Thermodynamics of Fluid-Phase Equilibria*; 1998.
- (26) Chapman, W. G.; Gubbins, K. E.; Jackson, G.; Radosz, M. SAFT: Equation-of-State Solution Model for Associating Fluids. *Fluid Phase Equilib.* **1989**, *52*, 31–38.
- (27) Chapman, W. G.; Gubbins, K. E.; Jackson, G.; Radosz, M. New Reference Equation of State for Associating Liquids. *Ind. Eng. Chem. Res.* **1990**, *29*, 1709–1721.
- (28) Wertheim, M. S. Fluids with Highly Directional Attractive Forces. I. Statistical Thermodynamics. *J. Stat. Phys.* **1984**, *35*, 19–34.
- (29) Wertheim, M. S. Fluids with Highly Directional Attractive Forces. II. Thermodynamic Perturbation Theory and Integral Equations. *J. Stat. Phys.* **1984**, *35*, 35–47.
- (30) Wertheim, M. S. Fluids with Highly Directional Attractive Forces. III. Multiple Attraction Sites. *J. Stat. Phys.* **1986**, *42*, 459–476.
- (31) Wertheim, M. S. Fluids with Highly Directional Attractive Forces. IV. Equilibrium Polymerization. *J. Stat. Phys.* **1986**, *42*, 477–492.
- (32) Vargas, F. M.; Garcia-Bermudes, M.; Boggara, M.; Punnapala, S.; Abutaqiya, M. I. L.; Mathew, N.; Prasad, S.; Khaleel, A. T.; AlRashed, M.; AlAsafen, H. On the Development of an Enhanced Method to Predict Asphaltene Precipitation. *Offshore Technol. Conf.* **2014**.
- (33) AlHammadi, A. A.; Chapman, W. G. Modeling the Polystyrene–Asphaltenes–Toluene Mixture Using the Perturbed-Chain Form of Statistical Associating Fluid Theory Equation of State. *Energy Fuels* **2017**, *31*, 6019–6024.
- (34) Alhammadi, A. A.; Alblooshi, A. M. Role of Characterization in the Accuracy of PC-SAFT Equation of State Modeling of Asphaltenes Phase Behavior. *Ind. Eng. Chem. Res.* **2019**, *58*, 18345–18354.
- (35) Panuganti, S. R.; Vargas, F. M.; Gonzalez, D. L.; Kurup, A. S.; Chapman, W. G. PC-SAFT Characterization of Crude Oils and Modeling of Asphaltene Phase Behavior. *Fuel* **2012**, *93*, 658–669.
- (36) Gonzalez, D. L.; Ting, P. D.; Hirasaki, G. J.; Chapman, W. G. Prediction of Asphaltene Instability under Gas Injection with the PC-SAFT Equation of State. *Energy Fuels* **2005**, *19*, 1230–1234.
- (37) Alhammadi, A. A.; Chen, Y.; Yen, A.; Wang, J.; Creek, J. L.; Vargas, F. M.; Chapman, W. G. Effect of the Gas Composition and Gas/Oil Ratio on Asphaltene Deposition. *Energy Fuels* **2017**, *31*, 3610–3619.
- (38) Cho, S. H.; Lee, B. S.; Byun, H. S. Phase Behavior of Tetrahydrofurfuryl Methacrylate and Poly (Tetrahydrofurfuryl

Methacrylate) in Supercritical Carbon Dioxide. *J. CO₂ Util.* **2018**, *25*, 39–45.

(39) Gross, J.; Sadowski, G. Perturbed-Chain SAFT: An Equation of State Based on a Perturbation Theory for Chain Molecules. *Ind. Eng. Chem. Res.* **2001**, *40*, 1244–1260.

(40) Fouad, W.; Haghmoradi, A.; Wang, L.; Bansal, A.; Al Hammadi, A.; Asthagiri, D.; Djamali, E.; Cox, K. R.; Chapman, W. G. Extensions of the SAFT Model for Complex Association in the Bulk and Interface. *Fluid Phase Equilib.* **2016**, *416*, 62–71.

(41) Nickmand, Z.; Aghamiri, F.; Aghamiri, S. F. A New Association Term for SAFT Equation of State. *J. Dispersion Sci. Technol.* **2010**, *31*, 1591–1599.

(42) Li, X. S.; Englezos, P. Vapor-Liquid Equilibrium of Systems Containing Alcohols Using the Statistical Associating Fluid Theory Equation of State. *Ind. Eng. Chem. Res.* **2003**, *42*, 4953–4961.

(43) Aghaie, M.; Rezaei, N.; Zendehboudi, S. Assessment of Carbon Dioxide Solubility in Ionic Liquid/Toluene/Water Systems by Extended PR and PC-SAFT EOSs: Carbon Capture Implication. *J. Mol. Liq.* **2019**, *275*, 323–337.

(44) Kondori, J.; Zendehboudi, S.; James, L. Evaluation of Gas Hydrate Formation Temperature for Gas/Water/Salt/Alcohol Systems: Utilization of Extended UNIQUAC Model and PC-SAFT Equation of State. *Ind. Eng. Chem. Res.* **2018**, *57*, 13833–13855.

(45) Ting, P. D.; Gonzalez, D. L.; Hirasaki, G. J. Application of the PC-SAFT Equation of State to Asphaltene Phase Behavior. *Asph. Heavy Oils Pet. Springer N. Y. NY* **2007**, 301–327.

(46) Economou, I. G. Statistical Associating Fluid Theory: A Successful Model for the Calculation of Thermodynamic and Phase Equilibrium Properties of Complex Fluid Mixtures. *Ind. Eng. Chem. Res.* **2002**, *41*, 953–962.

(47) Fu, Y.-H.; Sandler, S. I. A Simplified SAFT Equation of State for Associating Compounds and Mixtures. *Ind. Eng. Chem. Res.* **1995**, *34*, 1897–1909.

(48) Gil-Villegas, A.; Galindo, A.; Whitehead, P. J.; Mills, S. J.; Jackson, G.; Burgess, A. N. Statistical Associating Fluid Theory for Chain Molecules with Attractive Potentials of Variable Range. *J. Chem. Phys.* **1997**, *106*, 4168–4186.

(49) Davies, L. A.; Gil-Villegas, A.; Jackson, G. Describing the Properties of Chains of Segments Interacting Via Soft-Core Potentials of Variable Range with the SAFT-VR Approach. *Int. J. Thermophys.* **1998**, *19*, 675–686.

(50) Tamouza, S.; Passarello, J.-P.; Tobaly, P.; de Hemptinne, J.-C. Group Contribution Method with SAFT EOS Applied to Vapor Liquid Equilibria of Various Hydrocarbon Series. *Fluid Phase Equilib.* **2004**, *222–223*, 67–76.

(51) VLXE|BLEND; VLXE ApS: Copenhagen, Denmark, 2018.

(52) Multiflash; KBC Advanced Technologies Ltd - A Yokogawa Company: United Kingdom, 2018.

(53) PVTsim; Calsep: Denmark, 2018.

(54) He, J.; Wang, B. Partition Coefficients of Methyl Methacrylate and Acetone between Polymer and Compressed Carbon Dioxide Phases by an in Situ Infrared Spectroscopy Method. *Ind. Eng. Chem. Res.* **2009**, *48*, 7354–7358.

(55) Dominik, A.; Chapman, W. G.; Kleiner, M.; Sadowski, G. Modeling of Polar Systems with the Perturbed-Chain SAFT Equation of State. Investigation of the Performance of Two Polar Terms. *Ind. Eng. Chem. Res.* **2005**, *44*, 6928–6938.

(56) AlHammadi, A. A.; Vargas, F. M.; Chapman, W. G. Comparison of Cubic-Plus-Association and Perturbed-Chain Statistical Associating Fluid Theory Methods for Modeling Asphaltene Phase Behavior and Pressure–Volume–Temperature Properties. *Energy Fuels* **2015**, *29*, 2864–2875.

(57) Gross, J.; Sadowski, G. Modeling Polymer Systems Using the Perturbed-Chain Statistical Associating Fluid Theory Equation of State. *Ind. Eng. Chem. Res.* **2002**, *41*, 1084–1093.

(58) Aida, T.; Aizawa, T.; Kanakubo, M.; Nanjo, H. Dependence of Volume Expansion on Alkyl Chain Length and the Existence of Branched Methyl Group of CO₂-Expanded Ketone Systems at 40° C. *J. Supercrit. Fluids* **2010**, *55*, 71–76.

(59) Sato, Y.; Yurugi, M.; Fujiwara, K.; Takishima, S.; Masuoka, H. Solubilities of Carbon Dioxide and Nitrogen in Polystyrene under High Temperature and Pressure. *Fluid Phase Equilib.* **1996**, *125*, 129–138.

(60) Gui, X.; Tang, Z.; Fei, W. Solubility of CO₂ in Alcohols, Glycols, Ethers, and Ketones at High Pressures from (288.15 to 318.15) K. *J. Chem. Eng. Data* **2011**, *56*, 2420–2429.

(61) Arya, A.; Liang, X.; von Solms, N.; Kontogeorgis, G. M. Modeling of Asphaltene Onset Precipitation Conditions with Cubic Plus Association (CPA) and Perturbed Chain Statistical Associating Fluid Theory (PC-SAFT) Equations of State. *Energy Fuels* **2016**, *30*, 6835–6852.

(62) Abutayy, M. I. L.; Sisco, C. J.; Vargas, F. M. A Linear Extrapolation of Normalized Cohesive Energy (LENCE) for Fast and Accurate Prediction of the Asphaltene Onset Pressure. *Fluid Phase Equilib.* **2019**, *483*, 52–69.